

Shock pressure multiplication in layered PVA + Al targets driven by a high-power laser pulse

S. Chaurasia^{1,*}, P. Leshma¹, J. Pasley²,
S. Tripathi¹ and M. Kumar³

¹High Pressure and Synchrotron Radiation Physics Division, and

³Radiation and Photochemistry Division,

Bhabha Atomic Research Centre, Trombay, Mumbai 400 085, India

²York Plasma Institute, Department of Physics, University of York, York, YO10 5DQ, UK

The results of laser-driven shock wave experiments for equation-of-state studies in layered targets (15 μm polyvinyl alcohol + 5 μm aluminum foil) using optical streak camera and multi-frame optical shadowgraphy-based diagnostics are presented. The experiment was performed on a 20 J, 300–800 ps Nd : glass laser system at the Bhabha Atomic Research Centre, Mumbai. The focused laser intensity on the targets was up to $5 \times 10^{14} \text{ W/cm}^2$. Use of the impedance mismatch technique enabled a shock pressure multiplication to be achieved in a 5 μm thick aluminum foil target coated with 15 μm thick polyvinyl alcohol ((C₂H₄O)_n) compared to an uncoated 5 μm thick aluminum target. The pressure amplification was independently measured using both an optical streak camera-based diagnostic and a multiframe optical shadowgraphy technique; the magnitude of the pressure amplification was determined to be 1.71–1.77X and 1.6–1.88X respectively. Supporting simulations were performed using the one-dimensional radiation hydrodynamics modelling code HYADES. In these simulations, we observed shock pressure multiplication of 1.68–1.72X in 5 μm thick Al when coated with 15 μm PVA, compared to a similar uncoated Al target.

Keywords: Equation-of-state studies, laser-pulse, layered targets, shock multiplication.

HIGH-power laser can shock materials up to Gbar pressure. Experiments conducted using direct/indirect laser irradiation of solid matter indicate that lasers are the most viable tools for generating extreme dynamic pressure loading. Cauble *et al.*¹ have produced a pressure of 0.75 Gbar using an X-ray-driven flyer to strike a stationary target. To simulate these experiments, which also exhibit features relevant to inertial confinement fusion (ICF)^{1–3}, geophysics, astrophysics^{4,5}, phase transformation studies⁶ and other areas of high energy density physics, requires knowledge of the equation-of-state (EOS) of the materials involved. The EOS defines the relationship between certain pairs of hydrodynamic quantities in a fluid, for instance between the pressure and density at a given entropy. From a knowledge of EOS it is possible to

deduce a set of Rankine–Hugoniot curves. A Rankine–Hugoniot curve is the locus of end conditions that may be reached by a single shock wave from a given initial state, and is important in understanding what conditions can be achieved by the passage of a single shock wave through a material. For high energy density physics studies, the relevant pressures that need to be accessed experimentally in order to investigate the EOS are much greater than those attainable by gas-guns and explosives and only a few datapoints are available from underground nuclear tests. With direct laser illumination, the shock pressures produced scale with the laser intensity. However, the planarity and the stability of the shock fronts as well as low preheating of the material ahead of the shock wave are essential to obtain accurate measurements of EOS. At higher laser intensity $>5 \times 10^{14} \text{ W/cm}^2$, nonlinear processes such as the parametric decay instability, stimulated Raman scattering and two-plasmon decay produce hot electrons that cause pre-heat of the target material. This in turn inhibits any meaningful measurement of EOS. To mitigate these effects, targets incorporating a low Z ablator are used to inhibit the generation of hard X-rays in experiments related to laser shock studies.

Interestingly, this also helps in producing high pressures (up to 50 Mbar) using a moderate intensity laser pulse in some multilayer targets. This is called the impedance mismatch technique. This technique enables shock pressures to be enhanced without the pitfalls associated with increasing the incident laser intensity^{7–10}. The technique has been applied to EOS measurements between 10 and 20 Mbar for Cu (ref. 10), Au (ref. 11) and low-density foams¹². In fact, the EOS of many materials between 10 and 20 Mbar have been determined using this technique in an indirect drive configuration¹³. It is possible for errors less than $\pm 3\%$ to be achieved.

In this communication, we present shock pressure enhancement in aluminum (Al) targets coated with polyvinyl alcohol (PVA) plastic. In the experiments we have used a novel multi-frame optical shadowgraphy technique to measure the free-surface velocity and an optical streak camera to measure the shock velocity independently. The shock pressure amplification calculated using both techniques independently in Al and PVA-coated Al is found to be similar and in agreement with numerical simulations performed using the HYADES radiation hydrodynamics code¹⁴.

The experiment was performed on a 20 J, 300–800 ps Nd : glass laser system at the Bhabha Atomic Research Centre, Mumbai¹⁵. This pulsed single-shot laser system consists of a commercial laser oscillator with an output energy of 100 mJ per pulse and a peak-to-background contrast of 10^5 . A chain of amplifiers following the oscillator increases the energy to 20 J and the focused laser intensity on the target ranges up to a few times 10^{14} W/cm^2 . The laser beam was focused on the target (T) using an $f/5$ plano-convex lens to a focal spot diameter of

*For correspondence. (e-mail: pgsivanand@gmail.com)

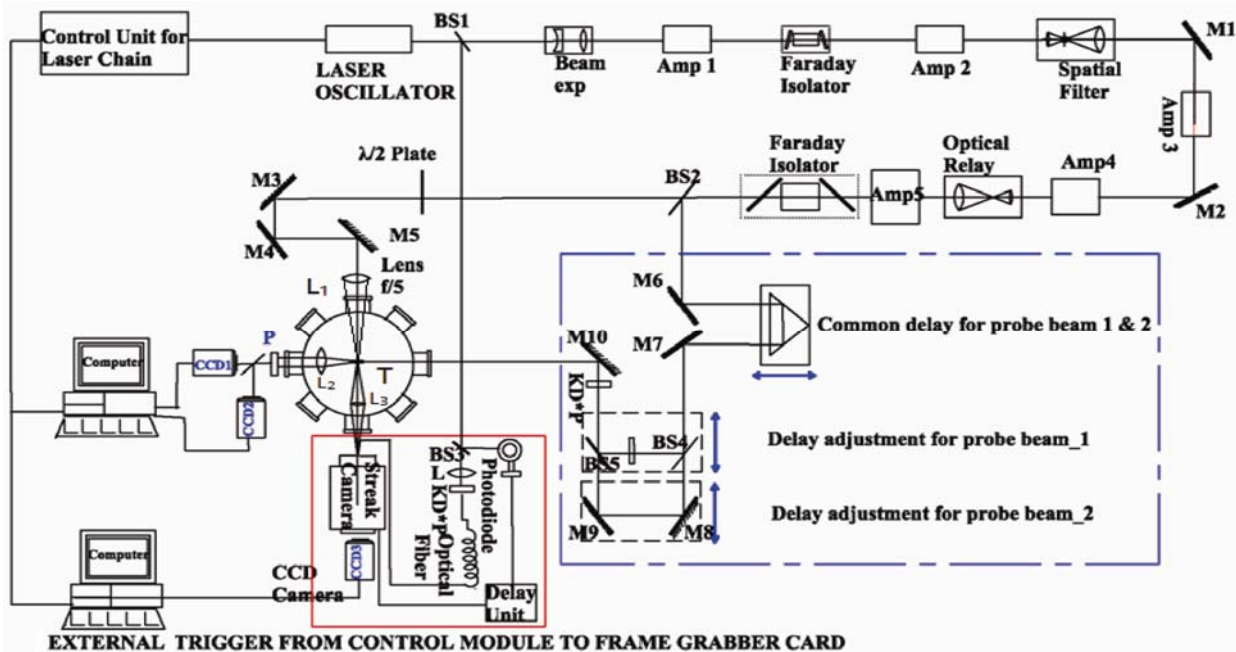


Figure 1. Schematic of the experimental set-up for shock velocity using an optical streak camera and free-surface velocity using two-frame optical shadowgraphy. The laser beam was focused onto the target T with an $f/5$ plano-convex lens L_1 . Lenses L_2 and L_3 were used to image the target onto the CCDs for the shadowgraphy and optical streak camera diagnostics respectively.

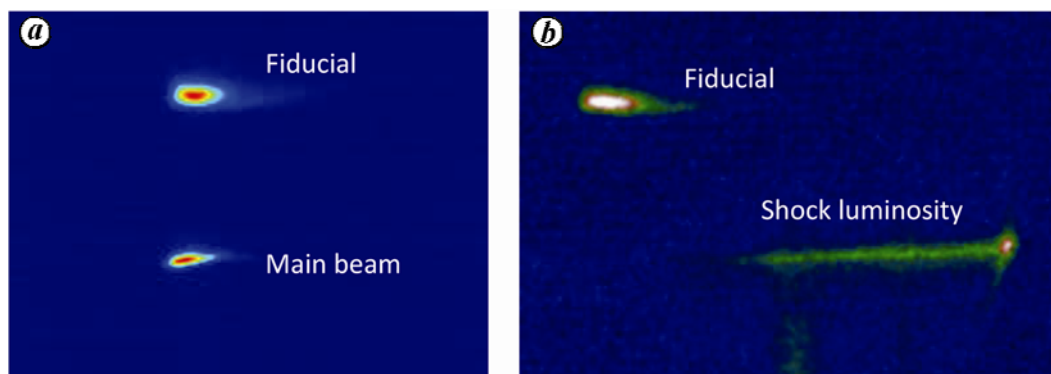


Figure 2. Shock velocity measurements. *a*, Synchronization of the main beam with the fiducial. *b*, Streak record of the fiducial and shock luminosity signals in 15 μm polyvinyl alcohol (PVA) + 5 μm aluminium (Al) foil at laser intensity of approximately $1 \times 10^{14} \text{ W/cm}^2$.

approximately 100 μm . The pulse shape is approximately Gaussian, with a FWHM of around 520 ps and a rise time of 375 ps. The shock transit time is obtained by determining the time interval between the arrival of the main laser pulse on the target and the onset of the shock luminosity at the rear of the target. The arrival of the laser pulse at the target is recorded on every shot by illuminating a portion of the streak camera slit with light from the drive laser using a fibre optic. A schematic of the set-up for the measurement of the shock transit time (shock velocity) and free surface velocity of target foils is shown in Figure 1. The synchronization of the main beam with a fiducial is shown in Figure 2*a*. The fiducial and the shock luminosity streak of the 5 μm Al is shown in

Figure 2*b*. Two-frame optical shadowgraphy is set up using a second harmonic backlighting probe beam. This probe is derived by extracting 1% of the laser light from the main beam at the final stage by introducing beam splitter BS2. An appropriate delay has to be introduced in its path using mirrors M6, M7 and a prism to record shadowgrams at desired delay times with respect to the main laser beam. Further, this beam is split into two parts with BS4, for the two shadowgram frames at two different delays. A polarizing beam-splitter is used to recombine these two beams again after a delay of 3.47 ns in one of the arms. These probe pulses then pass through the KD*P crystal and are converted to second harmonic (532 nm) for the shadowgraphy. They are propagated along the

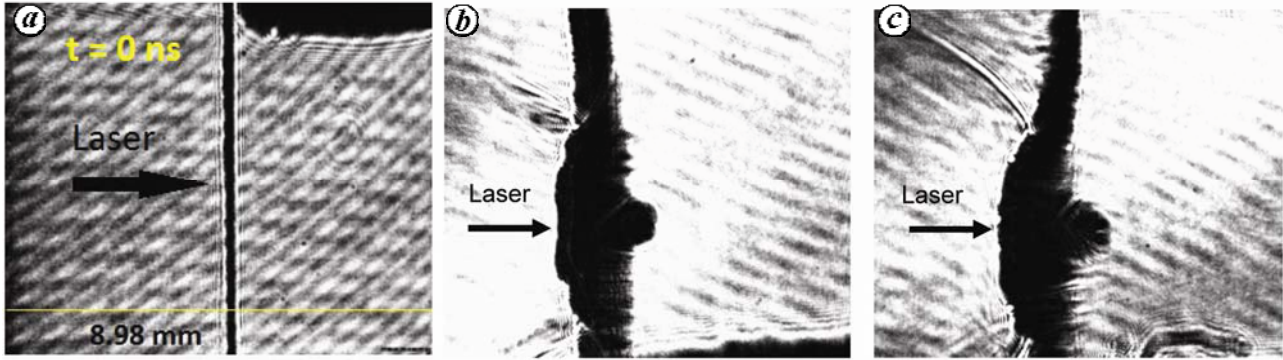


Figure 3. *a*, Shadowgraph recorded at $t = 0$ ns (unirradiated). *b*, *c*, Shadowgraph recorded at $t = 4.82$ ns for (*b*) $5\ \mu\text{m}$ Al foil irradiated with $9.37\ \text{J}/500\ \text{ps}$ laser and (*c*) $15\ \mu\text{m}$ PVA + $5\ \mu\text{m}$ Al foil irradiated with $9.32\ \text{J}/500\ \text{ps}$ laser on PVA side. The focal spot diameter is about $100\ \mu\text{m}$ in both cases.

Table 1. Values of constants a , b , and density of aluminum (Al) and polyvinyl alcohol

| Material | a | b | ρ_0 (g/cm ³) |
|----------|--------|-------|-------------------------------|
| Al | 0.5386 | 1.339 | 2.7 |
| PVA (CH) | 0.246 | 1.565 | 1.26 |

same optical path and illuminate the target edge such that the target foil is aligned at the centre of the field of view. After this, the two pulses are split again into two beams with the help of a polarizing beam-splitter and recorded with the cameras CCD1 and CCD2. Thus, in the present set-up, per laser shot, we can fix the time delay of each of the two frames independently. For the subsequent laser shots, a constant delay can be introduced in both the arms by introducing a delay of $1.9\ \text{ns}$ in the main shadowgraphy beam arm. In this set-up, the accuracy in delay between the two frames of the optical shadowgrams is $10\ \text{ps}$. Details of the development of multi-frame shadowgraphy systems and measurement of free surface velocities have been reported elsewhere^{16,17}. Experiments have been performed wherein foil motion is recorded in two laser shots of similar energy. In the first shot, the probe beam (PB) delays are fixed at 2.92 and $6.39\ \text{ns}$ with respect to the arrival of the main beam at the target and in the second shot the probe beam delays are changed to 4.82 and $8.29\ \text{ns}$. All these delays are measured with the help of a vacuum biplanar photodiode (rise time $80\ \text{ps}$) and are verified with the optical streak camera (temporal resolution $20\ \text{ps}$). The temporal resolution of the set-up is limited to $500\ \text{ps}$ by the probe pulse duration. The spatial resolution and image magnification of the shadowgraphy set up have been measured using a standard Air Force test target and are about 12 and $3.5\ \mu\text{m}$ respectively. The ultimate spatial resolution of the experimental set up is limited by the CCD camera pixel size of $6.45\ \mu\text{m}$. Typical shadowgrams recorded for $5\ \mu\text{m}$ thick Al and $15\ \mu\text{m}$ PVA + $5\ \mu\text{m}$ thick Al foil at a laser intensity of approximately $1 \times 10^{14}\ \text{W}/\text{cm}^2$ are shown in Figure 3 *a* and *b* respectively, for a delay of $4.82\ \text{ns}$.

The simulations were performed using the one-dimensional radiation hydrodynamics simulation code, HYADES¹⁴. HYADES is a three-temperature Lagrangian radiation hydrodynamics simulation code incorporating a flux-limited diffusion approximation for electron conduction and a multigroup diffusion treatment for radiation transport. In these simulations the flux limiter was set to a value of 0.05 , as is appropriate for 1ω illumination. The multigroup radiation diffusion model incorporated 40 groups, with group boundaries arranged logarithmically from $1\ \text{eV}$ to $2\ \text{keV}$. Tabulated EOS data from the SESAME library were employed to describe the hydrodynamic properties of Al and plastic layers.

When a laser pulse is focused onto the target foil, the surface gets ablated and a hot plasma is created which expands away from the target surface and exerts pressure on the foil. This leads to the formation of a strong shock wave, moving into the interior of the target, which changes the density and internal energy. Knowledge of pressure in the materials can be attained by measuring the shock velocity and particle velocity. We have measured the shock velocity using an optical streak camera and the particle velocity using the multi-frame optical shadowgraphy technique described earlier. Then we have calculated shock pressure independently from data provided by the streak camera record and shadowgraphy records. The Rankine–Hugoniot relations are used for shock velocity, particle velocity and shock pressure calculation as given below.

$$u_s = a + bu_p, \quad (1)$$

$$P - P_0 = \rho_0 u_s u_p, \quad (2)$$

where u_s , u_p , ρ_0 and P are the shock velocity, particle velocity, density of the material and pressure respectively, and both a and b are constants. The values of a , b and ρ_0 for Al and PVA are listed in Table 1.

In case of shock parameters measured using the optical streak camera, the shock transit times in $5\ \mu\text{m}$ Al and $15\ \mu\text{m}$ PVA + $5\ \mu\text{m}$ Al targets were $172\ \text{ps}/175\ \text{ps}$ and

RESEARCH COMMUNICATIONS

Table 2. Values of shock velocity, particle velocity and shock pressure as inferred from the streak camera records

| Thickness/targets | Shock transit time (ps) | Shock velocity ($\times 10^6$ cm/s) | Particle velocity ($\times 10^6$ cm/s) | Pressure (Mbar) |
|-------------------------------|-----------------------------------|--------------------------------------|---|-----------------|
| 5 μ m Al | 175 | 2.85 | 1.732 | 13.32 |
| 5 μ m Al | 172 | 2.90 | 1.76 | 13.78 |
| 15 μ m PVA | 289 | 5.19 | 3.15 | 20.5 |
| 15 μ m PVA + 5 μ m Al | 425 (transit time in Al – 135 ps) | 3.698 | 2.359 | 23.55 |

Table 3. Values of free-surface velocity, particle velocity, shock velocity and pressure as inferred from shadowgraphic measurements

| Thickness/targets | Free surface velocity ($\times 10^6$ cm/s) | Particle velocity ($\times 10^6$ cm/s) | Shock velocity ($\times 10^6$ cm/s) | Pressure (Mbar) |
|---------------------------|---|---|--------------------------------------|-----------------|
| 5 μ m Al | 3.599 | 1.7995 | 2.95 | 14.33 |
| 5 μ m Al | 3.75 | 1.875 | 3.04 | 15.36 |
| 5 μ m Al | 3.47 | 1.735 | 2.855 | 13.34 |
| 15 μ m PVA | 6.3 | 3.15 | 5.19 | 20.5 |
| (15 + 5 μ m) PVA + Al | 4.799 | 2.4 | 3.752 | 24.31 |
| (15 + 5 μ m) PVA + Al | 4.88 | 2.44 | 3.8057 | 25.1 |

425 ps respectively. Since the target thickness is known, we were able to calculate shock velocity in the 5 μ m Al foil. The shock transit time in PVA using the optical shadowgraphy technique was calculated to be 289 ps. So, the transit time across 5 μ m of Al in the layered target is 136 ps. Hence, the shock velocity and shock pressure calculated are 3.698×10^6 cm/s and 23.55 Mbar respectively. Details of shock velocity, particle velocity and pressure are listed in Table 2. From Table 2 it can be seen that a shock pressure multiplication between 1.71 and 1.77 times is inferred in 5 μ m Al when coated with a layer of 15 μ m PVA. We have also performed pressure measurement in pure 5 μ m Al and 15 μ m PVA + 5 μ m Al targets using multi-frame optical shadowgraphy. The free surface velocity of 5 μ m Al and 15 μ m PVA + 5 μ m Al targets was measured at four different delays with respect to start of the main laser pulse on the target. The particle velocity u_p was calculated using the relation $u_p = u_{fs}$ (free surface velocity)/2. The shock velocity and shock pressure were calculated using eqs (1) and (2) and the values of a and b listed in Table 1. Details of the shock velocity, particle velocity and shock pressure for 5 μ m Al and 15 μ m PVA + 5 μ m Al are given in Table 3 at a fixed laser energy of 9.62 J. From Table 3 it can also be seen that with this diagnostics, a shock pressure multiplication factor of 1.63–1.88 relative to the 5 μ m Al foil is inferred when coated with a 15 μ m thick layer of PVA. The shock pressure calculated by the optical shadowgraphy technique shows results about 7% higher than the pressure measured from the streak camera measurement in both 5 μ m Al and 15 μ m PVA + 5 μ m Al. This can be explained on the basis of work published by Benuzzi-Mounaix *et al.*¹⁸. The free surface velocity is related to the fluid velocity (particle velocity) by

$$u_{fs} = u_p + \int_0^P \left(\frac{\partial(1/\rho)}{\partial P'} \right)^{1/2} dP' = u_p + u_{rw}, \quad (3)$$

where u_{rw} is the release wave coming back into compressed materials after the shock breaks out. In our case we have taken $u_{fs} = 2u_p$, which is applicable only in case of weak shock wave [i.e. $(1 - \rho_0/\rho) \ll 1$], where the entropy change is small, and $u_{rw} = u_p$. But for high pressure this value increases by 10–15% compared to SESAME data¹⁹ as reported by Benuzzi-Mounaix *et al.*¹⁸.

Simulation results are shown in Figure 4. The simulation was performed for a laser energy of 10 J in 500 ps pulse duration focused on the target in 200 μ m spot size. From the simulation result also, we observed shock pressure multiplication of 1.68–1.72X in 5 μ m Al when coated by 15 μ m PVA foil compared to pure 5 μ m Al.

The shock multiplication technique has been demonstrated in a PVA-coated Al target driven by a 10 J/500 ps laser pulse. Data were taken using an optical streak camera with a 20 ps resolution and multi-frame optical shadowgraphy with spatial and temporal resolution of 12 μ m and 500 ps respectively. The optical streak camera record shows that the multiplication in shock pressure in the layered PVA + Al target compared to a pure Al target is about 1.71–1.77 times. The shadowgraphy measurement shows a shock pressure multiplication in the layered targets of 1.63–1.88 times compared to the pure Al targets, as shown in Table 1. The ratio of the shock pressure in the PVA-coated Al target compared to the uncoated Al target is similar for both diagnostics, but the individual reading from the optical shadowgraphy is about 7% higher than the streak camera measurement. Theoretical simulations have been performed for the layered as well

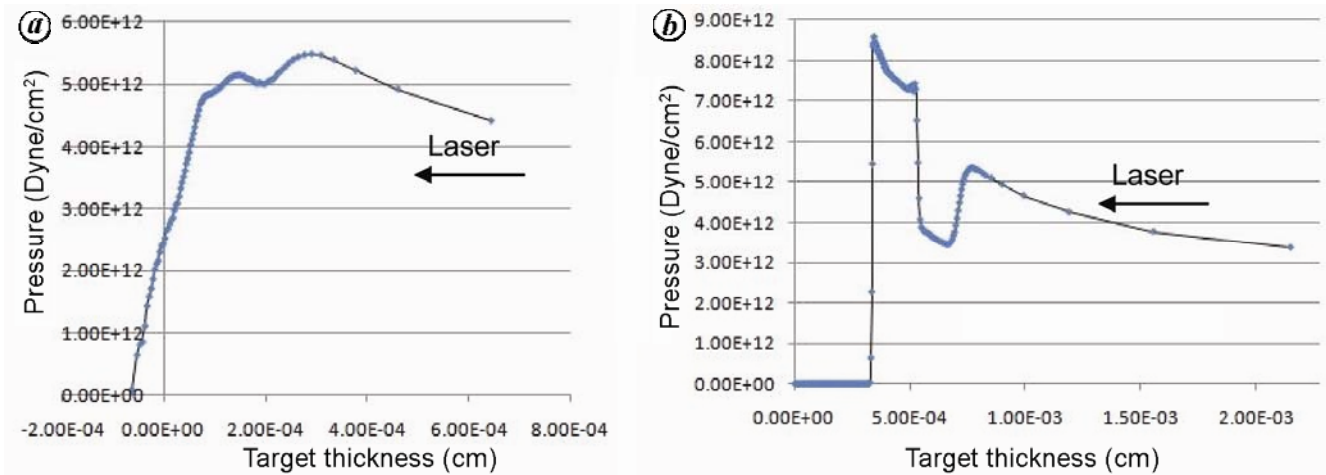


Figure 4. Theoretical simulation done using the HYADES radiation hydrodynamics simulation code at laser intensity of 6×10^{13} W/cm² (10 J, 500 ps, focal spot diameter \sim 200 μ m) for the shock pressure calculation in (a) 5 μ m thick Al foil and (b) 15 μ m thick PVA + 5 μ m thick Al foil.

as the pure targets. From the simulation of a 1.06 μ m laser with laser energy 10 J and pulse duration of 500 ps, with an effective focal diameter of 200 μ m at the target surface, the shock multiplication is observed to be 1.68–1.7 times.

1. Cauble, R., Phillion, D. W., Hoover, T. J., Holmes, N. C., Kilkenny, J. D. and Lee, R. W., Demonstration of 0.75 Gbar planar shocks in X-ray driven colliding foils. *Phys. Rev. Lett.*, 1993, **70**, 2102–2105.
2. Lindl, J., Development of the indirect-drive approach to inertial confinement fusion and the target physics basis for ignition and gain. *Phys. Plasmas*, 1995, **2**, 3933–4024.
3. Colliers, P. M. *et al.*, Shock-induced transformation of liquid deuterium into a metallic fluid. *Phys. Rev. Lett.*, 2000, **84**, 5564–5567.
4. Remington, B. A., Drake, R. P., Takabe, H. and Arnett, D., A review of astrophysics experiments on intense lasers. *Phys. Plasmas*, 2000, **7**, 1641–1652.
5. Remington, B. A., High energy density laboratory astrophysics. *Plasma Phys. Control. Fusion*, 2005, **47**, A191–A203.
6. Hicks, D. G., Boehly, T. R., Celliers, P. M., Eggert, J. H., Vianello, E., Meyerhofer, D. D. and Collins, G. W., Shock compression of quartz in the high-pressure fluid regime. *Phys. Plasmas*, 2005, **12**, 082702-1–7.
7. Batani, D. *et al.*, Optical smoothing for shock-wave generation: application to the measurement of equations of state. *Laser Part. Beams*, 1996, **14**, 211–223.
8. Koenig, M. *et al.*, Relative consistency of equations of state by laser driven shock waves. *Phys. Rev. Lett.*, 1995, **74**, 2260–2263.
9. Hall, T., Batani, D., Nazarov, W., Koenig, M. and Benuzzi, A., Recent advances in laser–plasma experiments using foams. *Laser Part. Beams*, 2002, **20**, 303–316.
10. Benuzzi, A. *et al.*, Indirect and direct laser driven shock waves and applications to copper equation of state measurements in the 10–40 Mbar pressure range. *Phys. Rev. E*, 1996, **54**, 2162–2165.
11. Batani, D. *et al.*, Equation of state data for gold in the pressure range <10 TPa. *Phys. Rev. B*, 2000, **61**, 9287–9294.
12. Koenig, M., Benuzzi, A., Philippe, F., Batani, D., Hall, T., Grandjovan, N. and Nazarov, W., Equation of state data experiments for plastic foams using smoothed laser beams. *Phys. Plasmas*, 1999, **6**, 3296–3301.
13. Rothman, S. D., Evans, A. M., Horsfield, C. J., Graham, P. and Thomas, B. R., Impedance match equation of state experiments using indirectly laser-driven multimegabar shocks. *Phys. Plasmas*, 2002, **9**, 1721–1733.
14. Larsen, J. T. and Lane, S. M., HYADES – a plasma hydrodynamics code for dense plasma studies. *J. Quant. Spectrosc. Radiat. Transfer*, 1994, **51**, 179–186.
15. Chaurasia, S., Munda, D. S., Murali, C. G., Dhareshwar, L. J., Vijayan, R. and Narayan, B. S., Design, development, optimization of 40 GW/300–800 ps Nd : glass laser system and study of matter at extreme temperature and pressure. BARC Report BARC/2008/E/006, 2008.
16. Tripathi, S., Chaurasia, S., Leshma, P. and Dhareshwar, L. J., Dynamic imaging and hydrodynamics study of high velocity, laser accelerated thin film foil targets using multiframe optical shadowgraphy. *PRAMANA-J. Phys.*, 2012, doi: 10.1007/s12043-012-0347-9.
17. Chaurasia, S., Tripathi, S., Leshma, P., Pasley, J. and Kumar, M., Shock pressure measurements in polyvinyl alcohol (PVA) films using multi-frame optical shadowgraphy. *J. Phys.*, 2012, **377**, 0120542-1–4.
18. Benuzzi-Mounaix, A. *et al.*, Absolute equation of state measurements of iron using laser driven shocks. *Phys. Plasmas*, 2002, **9**, 2466–2469.
19. SESAME: the LANL equation of state database. Report LA-UR-92-3407, Los Alamos National Laboratory, USA, 1992.

ACKNOWLEDGEMENTS. We thank Dr S. M. Sharma, Head, High Pressure and Synchrotron Radiation Physics Division and Dr S. Kailas, Director of the Physics Group, BARC, Mumbai, for support and encouragement. We also thank C. G. Murali and Diwakar S. Munda for help in the design and implementation of laser electronics and smooth operation of the laser system. M.K. acknowledges the support received from Dr S. K. Sarkar, Head, RPCD, and Dr T. Mukherjee, Director of the Chemistry Group, BARC.

Received 15 March 2012; revised accepted 15 November 2012